Physics Letters B 778 (2018) 221–226

Contents lists available at ScienceDirect

Physics Letters B

www.elsevier.com/locate/physletb

Thermal dynamics on the lattice with exponentially improved accuracy

Jan M. Pawlowski [a,b], Alexander Rothkopf [a,*]

[a] Institute for Theoretical Physics, Universität Heidelberg, Philosophenweg 12, D-69120 Heidelberg, Germany
[b] ExtreMe Matter Institute EMMI, GSI, Planckstr. 1, D-64291 Darmstadt, Germany

ARTICLE INFO

Article history:
Received 25 April 2017
Received in revised form 10 January 2018
Accepted 16 January 2018
Available online 18 January 2018
Editor: J.-P. Blaizot

Keywords:
Thermal quantum field theory
Lattice simulations
Spectral functions

ABSTRACT

We present a novel simulation prescription for thermal quantum fields on a lattice that operates directly in imaginary frequency space. By distinguishing initial conditions from quantum dynamics it provides access to correlation functions also outside of the conventional Matsubara frequencies $\omega_n = 2\pi nT$. In particular it resolves their frequency dependence between $\omega = 0$ and $\omega_1 = 2\pi T$, where the thermal physics $\omega \sim T$ of e.g. transport phenomena is dominantly encoded. Real-time spectral functions are related to these correlators via an integral transform with rational kernel, so that their unfolding from the novel simulation data is exponentially improved compared to standard Euclidean simulations. We demonstrate this improvement within a non-trivial $0+1$-dimensional quantum mechanical toy-model and show that spectral features inaccessible in standard Euclidean simulations are quantitatively captured.

1. Introduction

Modern experiments ranging from heavy-ion collisions at RHIC and LHC [1,2] to ultracold quantum gases [3] explore the physics of strongly-correlated quantum systems across vastly separated temperature scales ($T \sim 10^{12}..10^{-9}K$) [4]. A unifying aspect of these studies are thermal phenomena. Among them the transport of conserved charges, in the form of e.g. shear [5–12] and bulk viscosities [13,14] or electric conductivities [15,16] is of particular interest. Another aspect is the in-medium modification of heavy bound states both in Quantum-Chromodynamics [17–21] and quantum-gases [22,23]. Connecting these aspects to fundamental interactions, such as QED and QCD, requires a thorough theoretical understanding of the equilibrium properties of quantum fields. Unfortunately in realistic experimental environments many approximate techniques, such as perturbation theory, are inapplicable and a non-perturbative numerical computation is required.

Conventional simulations of quantum fields, e.g. lattice QCD, are based on non-perturbative Monte-Carlo techniques, which rely on an analytic continuation of the real-time axis into the complex plane [24,25]. Alternative direct real-time approaches include 2PI techniques [26] as well as the Dyson–Schwinger [27] and Functional Renormalization Group approaches [7,8,28–34].

In order to extract real-time information from correlators simulated in Euclidean time a numerical analytic continuation via spectral functions is unavoidable. Two conceptual challenges exist: the most important one is the finite extent of the Euclidean time axis, denoted in the following by $\bar{\tau} \in [0\,,\, 1/T]$. It leads to discrete Matsubara frequencies $\omega_n = 2\pi nT$, which constitutes a limit to the resolution of imaginary frequencies. In turn, increasing the number of temporal points $N_{\bar{\tau}}$ decreases the temporal lattice spacing $a_{\bar{\tau}}$, thus increases the maximum imaginary frequency available, while keeping the frequency spacing fixed. Hence, a large $N_{\bar{\tau}}$ does not improve the access to the relevant regime of imaginary frequencies $\omega \sim T$, where thermal physics is dominantly encoded in the imaginary frequency correlator $G(\omega)$ (see Eq. (2)). The contributions of thermal effects to $G(\omega)$ actually decay rapidly above $\omega \approx T$ and already $G(\omega = \omega_1 = 2\pi T)$ may be dominated by $T = 0$ physics.

In order to resolve this conceptual issue, we present a simulation algorithm, which operates in imaginary frequency space with arbitrary resolution, given by the number of chosen imaginary frequency points N_ω. In particular this approach resolves frequencies between the standard ω_0 and ω_1.

The second issue concerns the unfolding of spectral functions $\rho(\mu)$ along real-time frequencies μ from Euclidean time correlators $G(\bar{\tau})$, or imaginary frequency correlators $G(\omega)$. For Euclidean time correlators the ensuing inverse problem reads

* Corresponding author.
E-mail address: rothkopf@thphys.uni-heidelberg.de (A. Rothkopf).

https://doi.org/10.1016/j.physletb.2018.01.037

$$G(\bar\tau) = \int_{-\infty}^{\infty} d\mu\, \tilde K(\mu,\bar\tau,T)\rho(\mu)$$

$$\tilde K(\mu,\bar\tau,T) = \frac{e^{-\mu\bar\tau}}{1-e^{-\mu/T}}, \quad \tilde K(\mu,\bar\tau,T) \overset{\mu\bar\tau>>1}{\sim} e^{-\mu\bar\tau}\,. \tag{1}$$

Eq. (1) leads to an exponentially hard ill-posed problem [35]. In this work we simulate directly in imaginary frequency space, where numerical data and spectral functions are related via the Källén–Lehmann kernel (resolvent),

$$G(\omega) = \int_{-\infty}^{\infty} d\mu\, K(\mu,\omega)\rho(\mu), \quad K(\mu,\omega) = \frac{1}{i\omega-\mu},$$

$$|K(\mu,\omega)| \overset{\mu/\omega>>1}{\sim} \frac{1}{\mu/\omega}\,. \tag{2}$$

This kernel does not suppress spectral information in the correlator exponentially, it is instead a rational function.[1] Since the finite lattice spacing provides a natural UV cutoff Eq. (2) in practice does not suffer from the relatively weak falloff of K. Instead, inverting Eq. (2) promises significantly improved results already using standard simulation data on the Matsubara frequencies $\omega = \omega_n$. Note that the kernel of Eq. (1) is simply the discrete Fourier transform of the Källén–Lehmann kernel in case that $\omega = \omega_n$ is evaluated at the Matsubara frequencies.

By computing $G(\omega)$ from a linear combination of the datapoints $G(\bar\tau)$ with complex Fourier coefficients, one obtains the kernel of Eq. (2), which is of Breit–Wigner form and thus peaked and local. From this point of view using Eq. (2) constitutes an analytic implementation of the idea behind the Backus–Gilbert [36] or Sumudu [37] approaches.

In summary, it is the combination of the rational kernel in (2) and the access to arbitrary frequencies that leads to exponentially improved accuracy in the spectral reconstruction, as demonstrated in Sec. 3 and Fig. 4.

2. Improved setup

Now we discuss the lattice setup that implements the above ideas. The starting point is a real-time thermal field theory, formulated on a modified Schwinger–Keldysh like contour [38,39]. It amounts to an initial value problem with the following path integral representation for the partition function

$$\mathcal{Z} = \underbrace{\int_{\varphi_E(0)=\varphi_E(\beta)} \mathcal{D}\varphi_E e^{-S_E[\varphi_E]}}_{\text{initial conditions}} \underbrace{\int_{\varphi^+(t_0,\mathbf{x})=\varphi_E(0)}^{\varphi^-(t_0,\mathbf{x})=\varphi_E(\beta)} \mathcal{D}\varphi e^{iS_M[\varphi^+]-iS_M[\varphi^-]}}_{\text{quantum dynamics}}, \tag{3}$$

with S_E being the Euclidean- and S_M the Minkowski space action. The field lives on the forward and backward branch, i.e. $\varphi^+(t,\mathbf{x})$ lives on the forward branch from the initial time $t = t_0 = -\infty$ to $t = \infty$, and $\varphi^-(t,\mathbf{x})$ lives on the backward branch, see Fig. 1. The initial conditions are expressed as a path integral for $\varphi_E(\bar\tau,\mathbf{x})$ on the compact imaginary time axis $\bar\tau \in [0,\beta]$. We find that, as shown in Sec. 3, the unconventional identification $\varphi_E(0) = \varphi_E(\beta)$ leads to sensible results, a more formal justification of this choice, applicable for infinitely extended real-time branches is work in progress.

[1] Just as in the case of the Euclidean kernel, the approach to the continuum limit and thus the emergence of UV divergences needs to be handled by an appropriate renormalization procedure.

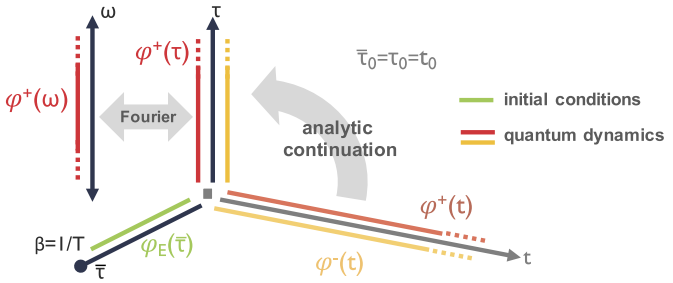

Fig. 1. Sketch of the novel setup. We distinguish between the conventional compact Euclidean time $\bar\tau$, Minkowski real-time t and a novel non-compact imaginary time axis denoted by τ. Imaginary frequencies are denoted by ω in contrast to real-time frequencies of spectral functions, which in the text read μ. (For interpretation of the references to color in this figure, the reader is referred to the web version of this article.)

The real-time contour extends to positive infinity, hence the final point at which forward and backward branch were originally connected has no correlation with any field at finite time t and we consider the branches as effectively cut open. In turn we rotate the real-time contour to an imaginary time axis denoted by τ, not to be confused with the Euclidean time axis of the initial condition path integral $\bar\tau$. To preserve normalization we rotate both branches to the upper complex half plane which results in a real and bounded measure for the forward path (see Fig. 1).

What distinguishes equilibrium from non-equilibrium settings is that $\rho(\mu)$ can be determined using only the fields on the forward branch, i.e. the correlator G in (2) is

$$G^{++}(\omega) := \langle \varphi^+(\omega)\varphi^+(-\omega)\rangle = \int_{-\infty}^{\infty} \frac{\rho(\mu)}{i\omega-\mu} d\mu\,. \tag{4}$$

Thus it suffices to compute the correlation functions on the forward contour, and we do not consider the decoupled backward contour any further here. The forward branch may now be treated using stochastic quantization [40] with a Euclidean action S_E. It receives information about temperature from the Euclidean field $\varphi_E(\bar\tau = 0)$, to which it is still coupled. The correlation function $G(\omega)$ can then be computed for all $\omega \in \mathbb{R}$.

One possibility is to discretize the analytically continued real-time contours directly in the non-compact imaginary time τ. In practice on a finite computer boundary conditions need to be supplied. All explicit b.c. we tested lead to correlators that differ from those of the standard simulation, even in the free case. This deviation we classify as a finite volume artifact, since we have checked that toward the infinite volume, i.e. the $\tau \to \infty$ limit, the correct correlator is approached, albeit only very slowly. We found that the convergence to the correct result can be significantly improved if instead the kinetic term is directly evaluated in imaginary frequency space, where it is local and one does not need to specify any boundary conditions for the free case.

This can be understood as follows: the Fourier transform to frequency space translates the thermal initial condition to the constraint $\sum_l \varphi^+(\omega_l) = \varphi_E(\bar\tau_0)$, where $|l| = 0,\dots,\lfloor N_\omega/2\rfloor$, and $\omega_l = 2\pi l/(N_\omega a_{\bar\tau})$. Here $a_{\bar\tau} = 1/N_{\bar\tau}T$ is the temporal lattice spacing on the standard Euclidean lattice. This constraint can be rewritten as one for the new φ^+ field at the highest frequency, $\varphi^+(\omega_{\lfloor N_\omega/2\rfloor}) = \varphi_E(\bar\tau_0) - \sum_l \varphi^+(\omega_l)$. The kinetic term $1/2\sum_l \varphi^+(\omega_l)\mathcal{P}(\omega_l)\varphi^+(\omega_l)$ with lattice dispersion $\mathcal{P}$ is local in frequency space. Note first that the constraint is irrelevant in the continuum limit, as its statistical weight is vanishing due to $\varphi^+(\omega_{\lfloor N_\omega/2\rfloor})\mathcal{P}(\omega_{\lfloor N_\omega/2\rfloor})\varphi^+(\omega_{\lfloor N_\omega/2\rfloor}) \to \infty$. Secondly, in the infinite volume we have an infinite number of momentum modes. This entails that the weight of one specific momentum mode tends towards zero. In summary, the dependence